MEMOIRS OF THE SCHOOL OF ENGINEERING, OKAYAMA UNIVERSITY, Vol. 8, No.2, December 1973

Dynamic Behaviour of Attaching Jet

Tsutomu WADA*, Akira SHIMIZU*, and Shujiro DOHTA**

(Received November 17, 1973)

Synopsis

The dynamic behaviour of attaching jet with single side wall to step control flow and the switching process of the bistable amplifiers were investigated experimentally and theoretically.

In the experiments, a large scale model was used with water. The flow patterns were visualized by the tracer of polystrene granules and were recorded by a cinecamera. In the analysis, the quasi-steady process was assumed.

The results obtained can be summarized as follows:

1) The proposed analytical dynamic model of attaching jet explains well the dynamic behaviour of attaching jet with single side wall.

2) The process of the opposite wall switching may be divided into three phases.

3) The analytical model of the opposite wall switching, including the formulation of the switching criterion, was proposed.

1. Introduction

Many works have been done on the dynamics of bistable wall attachment fluid amplifier. Some of them include papers by Müller [1], Lush [2], and Epstein [3], which were studied on the end wall switching.

* Department of Industrial Science

** Graduate Student, Department of Industrial Science

Of several types of switching possible in bistable fluid amplifiers, the opposite wall switching is considered to be the most fundamental and most important type [4]. Hence, it is necessary to formulate the switching process, especially the dynamic one, of this type.

However, such process was analyzed theoretically by Özgü [5] only. His theory puts stress on the process that the main jet moves downstream attaching on both side walls. It seems that this theory can be applied phenomenally in case of small offset or relatively large input. But this lacks generality in explaining the mechanism of the opposite wall switching, because this does not consider the influence of the opposite wall on the attaching jet, i.e. lowering of static pressure in opposite side. So, more reasonable theory is required.

Therefore, mainly by means of flow visualization, the dynamic behaviour of attaching jet to step control flow is investigated experimentally and theoretically.

First, for a model of the fluidic device with single side wall, the analytical dynamic model of attaching jet is proposed based on the statical analysis. And this theory is compared with the experimental results.

Next, after making clear the mechanism of the opposite wall switching by experiments and discussing the problems in formulating the process, an analytical model is proposed, which includes the switching criterion.

2. Experimental Setup and Method

Fig.1 shows the large scale model used for experiments. In order to simplify an analytical model, this model has no splitter and suf-

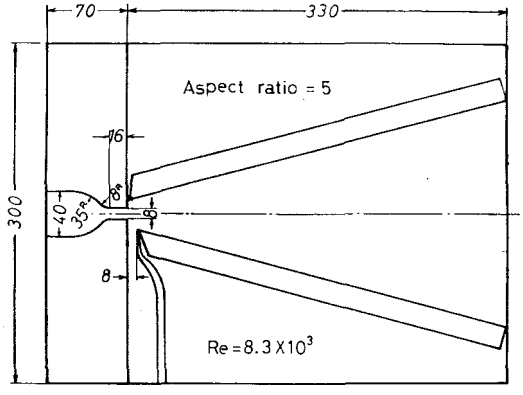

Fig.1 Large scale model

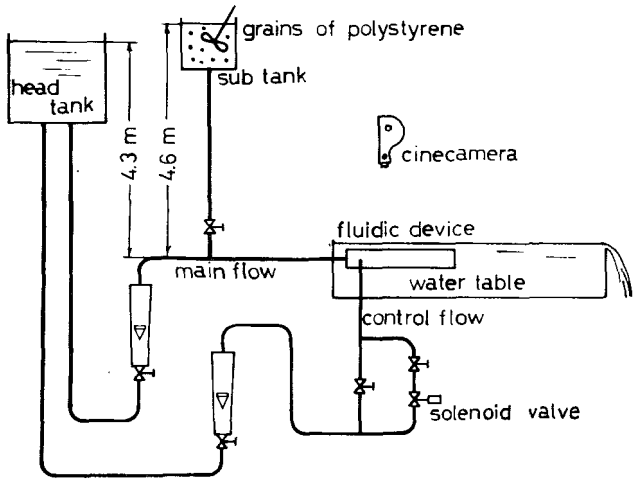

Fig.2 Schematic diagram of experimental set-up

ficiently long walls compared with its attachment distance. The experimental setup is shown in Fig.2. All experiments are carried out with water. Reynolds number of the jet was 8300 using the main nozzle width as the characteristic length. Pressure changes in several points in the flow field are measured by mini-pressure transducers and are recorded by the electro-magnetic oscillograph. A step-wise change in the control flow is applied by a solenoid valve.

In order to observe the dynamic behaviour of the jet in switching process, the polystrene granules are mixed into the main jet as the tracer for flow visualization. The granules are 0.5 - 0.8 mm in diameter and have the same specific gravity as water. The attachment distance and the deflection angle of jet are evaluated by photographs, obtained by a 16 mm cinecamera.

3. Dynamic Behaviour of Jet with Single Side Wall

3.1. Theoretical Analysis

The theory is based on the statical analysis of attaching jet [6]. The analytical model is shown in Fig.3. In this analysis, the following assumptions are added to those used usually [6].

(a) The growth of the separation bubble is treated as a quasi-steady process.

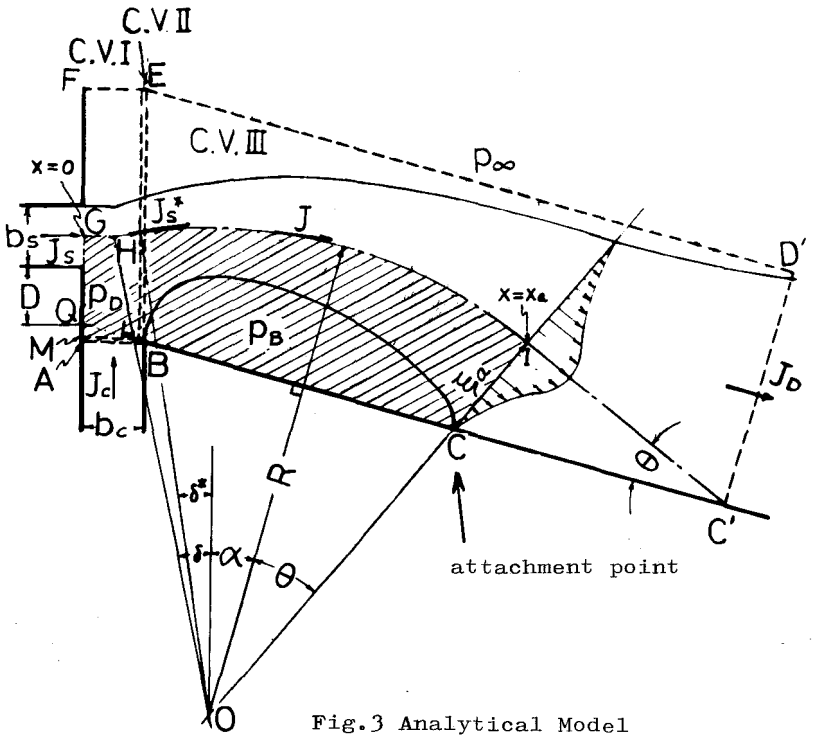

Fig.3 Analytical Model

(b) The separation bubble is defined as the region enclosed by the jet centerline and the bounding walls, shaded region in Fig.3.

Further, all variables in equations are non-dimensionalized under the condition of the constant supply flow, because the use of the pressure source could not be realized in experiments.

Momentum Balance

Three control volumes (C.V. in short) are considered as shown in Fig.3. Considering C.V.I, the momentum equations are

$$J \sin\delta^* = J_c + p_D b_c, \tag{1}$$

and

$$J \cos\delta^* \simeq J_s, \tag{2}$$

where $J_s = \rho Q_s^2/b_s = 2\alpha_s^2 p_{so} b_s$

and $J_c = \rho Q_c^2/b_c = 2\alpha_c^2 (p_c - p_D) b_c$.

From C.V.II, the following equation is obtained,

$$(J - J_s^*)\cos\delta^* = (p_D - p_B)D^*. \tag{3}$$

In above three equations, Eq.(1) - Eq.(3), the quantities, J, J_s^*, δ^* and p_D are unknown, and p_B is obtained by the other relations. In addition, therefore, one equation is necessary. It is assumed that the jet momentum in flow direction increases suddenly at the section BE.

Then, the increment $J-J_s^*$ may be represented as follows:

$$J - J_s^* = J_c + 2\lambda(p_D - p_B)b_c. \tag{4}$$

λ is an exchange factor, by which the pressure in interaction region is exchanged into the momentum downstream.

From Eq.(1) and Eq.(2), we obtain in non-dimensionalized form,

$$\tan\delta^* = \bar{Q}_c^2/\bar{b}_c + \bar{p}_D\bar{b}_c/(2\alpha_s^2). \tag{5}$$

Considering the time required during the deflection of the jet, Eq.(1) is assumed to have following meanings:

$$\tan\delta^* = \bar{p}_D\bar{b}_c/(2\alpha_s^2) \qquad (\tau = 0^- = 0)$$
$$= \bar{Q}_c^2/\bar{b}_c + \bar{p}_D\bar{b}_c/(2\alpha_s^2). \quad (\tau \geqq 0^+)$$

Using Simson's velocity profile of the free jet, the momentum J_d becomes as followings:

$$J_d = J_{os} + 0.734\ u_m^2 b_a + 0.266\ u_m^2 b_t\ .$$

Since $J_{os}=P_{so}(1 + \bar{p}_D/4)b_s\alpha_s^2$, the above equation can be written in a non-dimensional form:

$$\bar{J}_d = (1 + \bar{p}_D/4)/2 + 0.734\bar{u}_m^2\bar{b}_a + 0.266\bar{u}_m^2\bar{b}_t. \tag{6}$$

Assuming $J_s^* \simeq J_s$ in Eq.3, the combined jet momentum J is given by

$$\bar{J} = 1 + \bar{Q}_c^2/\bar{b}_c + \lambda(\bar{p}_D - \bar{p}_B)\bar{b}_c/\alpha_s^2. \tag{7}$$

From Eq.(4) and Eq.(7), we obtain a following equation:

$$\bar{p}_D - \bar{p}_B = \alpha_s^2 \frac{\bar{Q}_c^2/\bar{b}_c}{\bar{D}^*/(2\cos\delta^*) - \lambda\bar{b}_c}\ , \tag{8}$$

Finally, considering C.V.III, the momentum equation is

$$J_d - J\cos(\alpha + \delta^*) = D^* p_B \cos\alpha\ ,$$

So

$$\bar{p}_B = 2\alpha_s^2 \frac{\bar{J}_d - \bar{J}\cos(\alpha + \delta^*)}{D^*\cos\alpha}\ . \tag{9}$$

By the usual assumption, the equation, $J/R = -p_B$, is obtained. The radius of curvature of jet centerline R is expressed with non-dimensional form as

$$\bar{R} = -2\alpha_s^2 \bar{J}/\bar{p}_B. \tag{10}$$

Geometrical Relations

By referring to Fig.3, the virtual impingement angle of jet to the side wall may be given by

$$\cos\Theta = \frac{\bar{R}\cos(\alpha + \delta) - \bar{D}^*\cos\alpha}{\bar{R} - \bar{\xi}_a}\ , \tag{11}$$

where ξ_a is the jet width on the attachment point, $x=x_a$, and is given by

$$\bar{\xi}_a = 2.02(\bar{b}_a - \bar{b}_t) + \bar{b}_t,$$

and $\delta \simeq \delta^* + \bar{b}_c/(2\bar{R})$.

The distance from the nozzle exit to the point above the attachment

point along the jet centerline is given by

$$\bar{x}_a = \bar{R}(\alpha + \theta + \delta) + \bar{b}_c/2. \qquad (12)$$

The distance from offset wall to the attachment point along the wall, that is, the attachment distance, is given by

$$\bar{x}_R = (\bar{R} - \bar{\xi}_a)\sin\theta + \bar{R}\sin(\alpha+\delta) + \bar{b}_c/2\cos\alpha - (0.5 + \bar{D})\sin\alpha .$$

Next, the volume of the separation bubble is defined as the region ABCÎHGA as shown in Fig.3, and is given by

$$V = \nabla OIH + \square GMLH - \Delta QML + \Delta QAB - \Delta OLC , \qquad (13)$$

where $\nabla OIH = R^2(\alpha + \theta + \delta)/2$,

$\square GMLH = \overline{HL}\cos\delta\,(b_c + \overline{HL}\sin\delta)/2$,

$\overline{HL} = R - \{(R - \xi_a)\cos\theta/\cos(\alpha+\delta)\}$,

$\Delta QML = (\overline{HL}\sin\delta + b_c/2)^2/2\tan\alpha$,

$\Delta QAB = b_c^2/2\tan\alpha$,

and $\Delta OLC = (R - \xi_a)^2/2\cos\theta\cdot\sin(\alpha+\delta+\theta)/\cos(\alpha+\delta)$.

Continuity

Referring to Fig.3, the rate of growth of the bubble is given by

$$\frac{dV}{dt} = Q_{in} - Q_{out} ,$$

which becomes

$$\frac{d\bar{V}}{d\tau} = \frac{1}{2}\sqrt{1 - \bar{p}_D/4} + \bar{Q}_c - \bar{u}_m\bar{b}_a , \qquad (14)$$

where following equations are used,

$$Q_{out} = u_m b_a ,$$

$$Q_{in} = Q_{is} + Q_c = \sqrt{P_{so}(1 - \bar{p}_D/4)/(2\rho)}\; b_s\alpha_s + Q_c$$

and $\tau = t\,u_s/b_s$.

3.2. Computational Procedures

Equations (5) through (14) constitute the complete set of equations necessary for the solution of the growing transient of the bubble. In Fig.4, the flow chart for computation is shown. Time t can be obtained by following integration:

$$t = \int_{V_o}^{V} \frac{dV}{(dV/dt)} \quad . \qquad (15)$$

In practical computation, time t can be obtained by the numerical integration using the half valued width b_a as a parameter. As a first step, the initial value of b_a is determined by Eq.(14) where dV/dt=0 and Q_c=0. Next, the deflection angle δ^* is increased by small amount, step by step, until Eq.(5) is satisfied. Then, b_a is increased by small amount. By this method the time required for deflection of jet

can be estimated [3]. Procedures mentioned above are repeated until the flow becomes the steady state: dV/dt=0. In this way, we can know the flow pattern at any time.

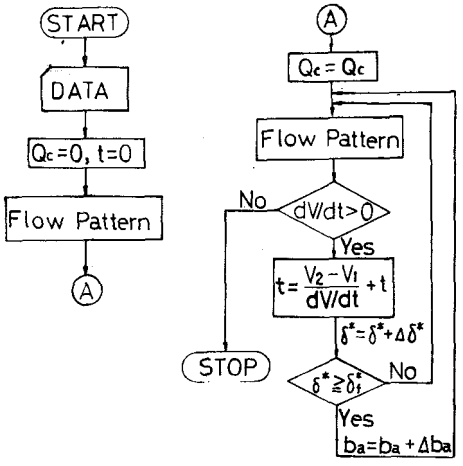

Fig.4 Flow chart

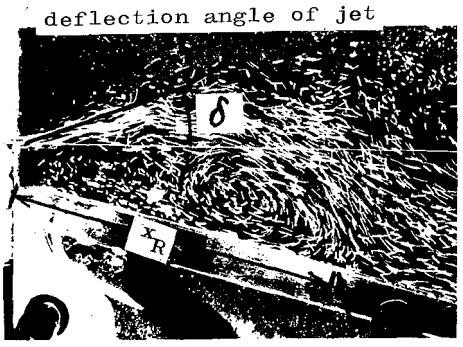

Photo.1 Definition of x_R and δ in photograph

3.3. Comparison with Experimental Results

In calculation the exchange factor λ =0.2 and the discharge coefficient of main nozzle α_s=1 are used. The simultaneous equations are solved in iteration process by the Newton's method.

Fig.5 shows the step response of the attachment distance x_R, and Fig.6 shows the step response of the deflection angle of jet δ. x_R and δ are measured as shown in Photo.1. The response records of the static pressure in interaction region p_D are shown in Fig.7, which are compared with theoretical results. In Photo.2, the calculated jet centerlines are compared with the flow pattern obtained by flow visualization. The proposed analytical model explains well the dynamic behaviour of attaching jet with single side wall.

4. Dynamic Behaviour of Jet in Switching

4.1. Switching Mechanism

Flow patterns of jet in switching is shown in Photo.3. Fig.8 shows the pressure changes in attaching side and in opposite one. By observing these behaviours of jet, it is seen that the opposite wall switching process can be divided into the following three phases: Phase 1 begins when a step change in the control flow is applied and ends when the switching criterion is satisfied.

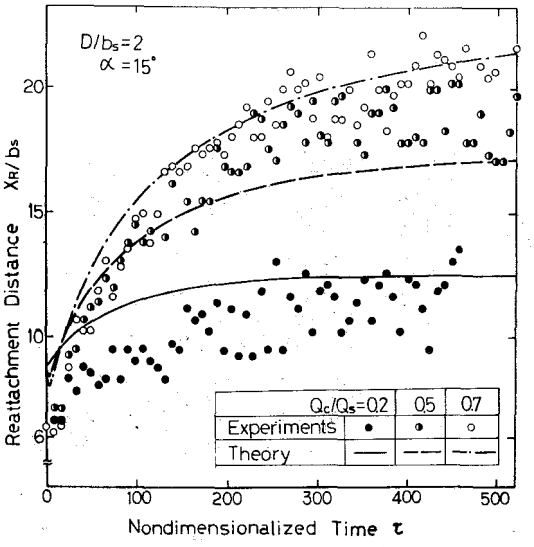

Fig.5 Step response of x_R

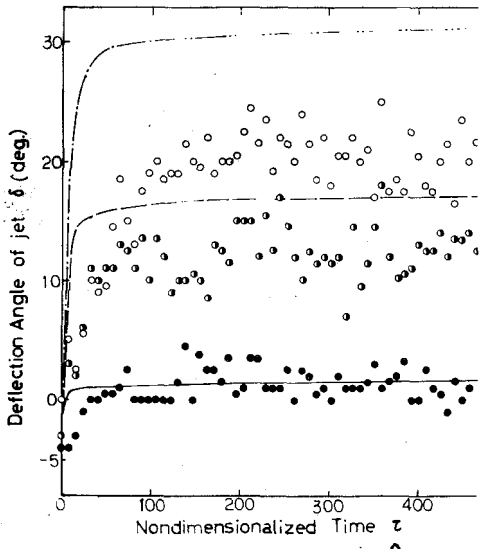

Fig.6 Step response of δ

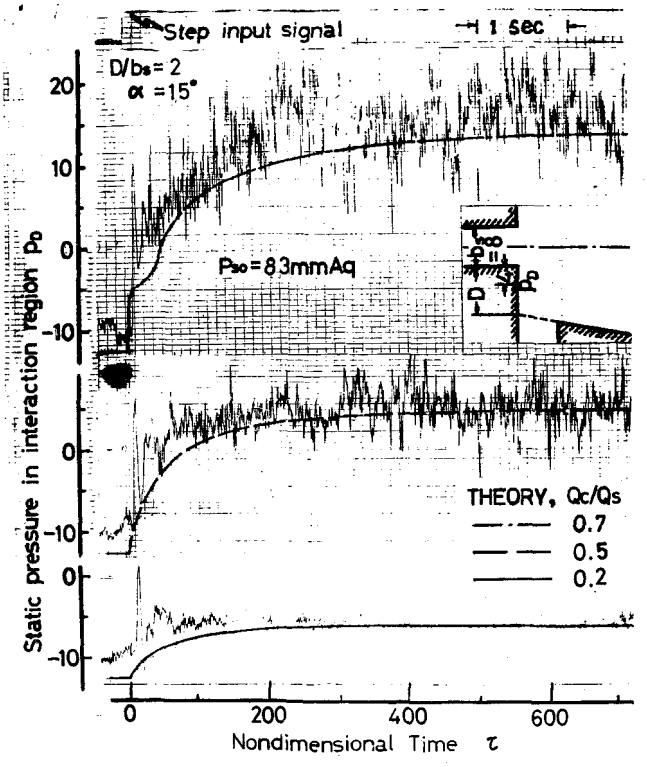

Fig.7 Step response of p_D

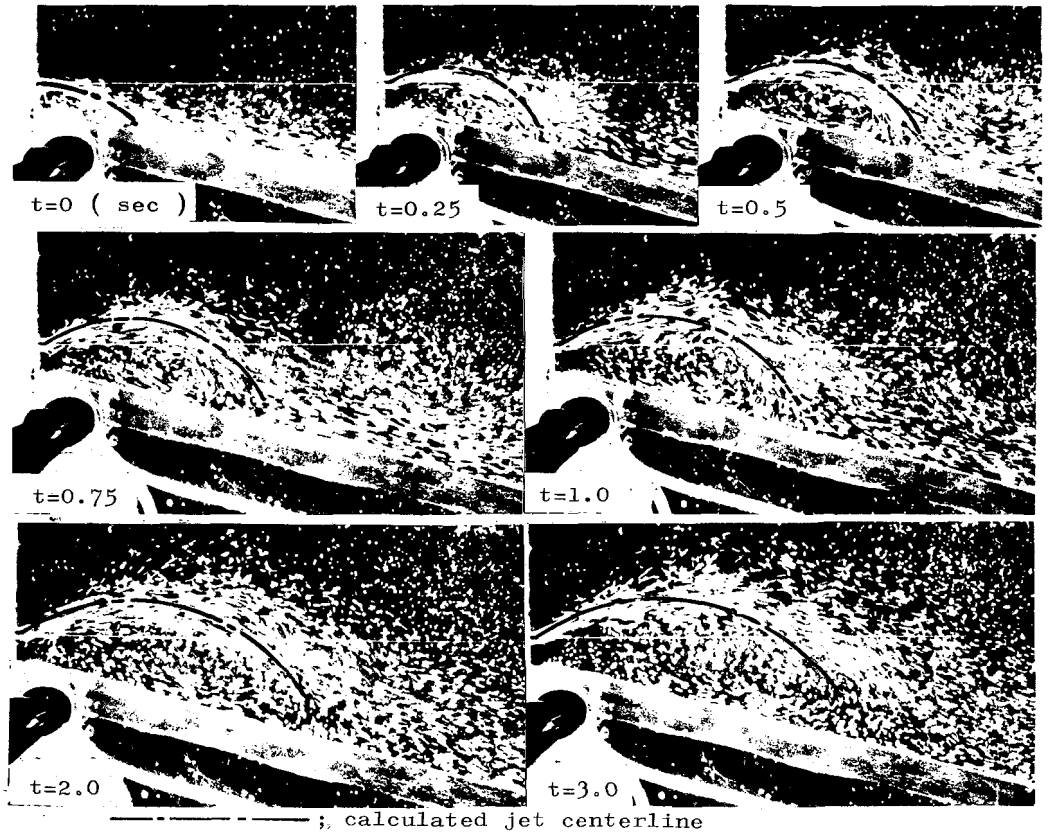

Photo.2 Flow patterns (Q_c/Q_s=0.7, D/b_s=1, α=15°)

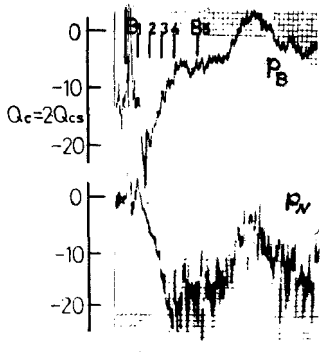

Fig.8(a) Response records in the opposite wall switching

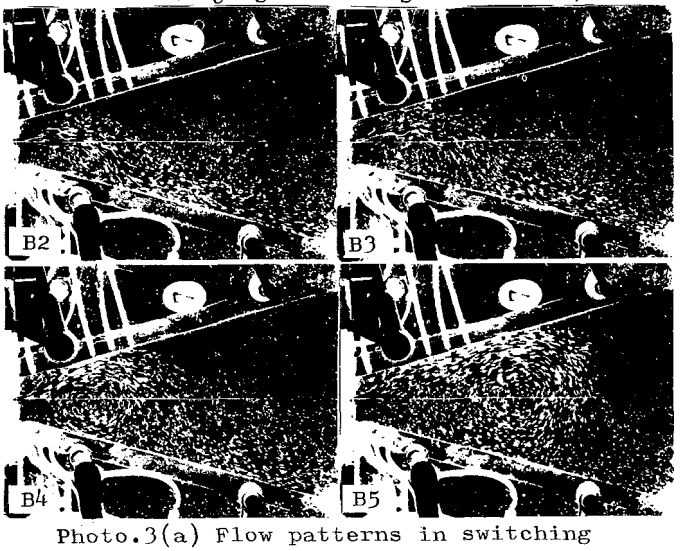

Photo.3(a) Flow patterns in switching

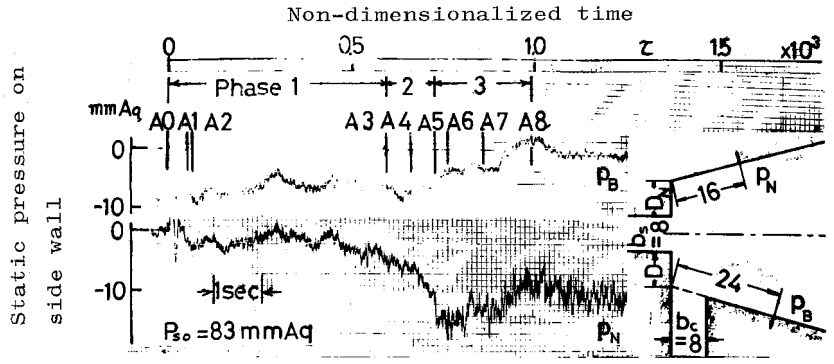

Fig.8(b) Response records in switching

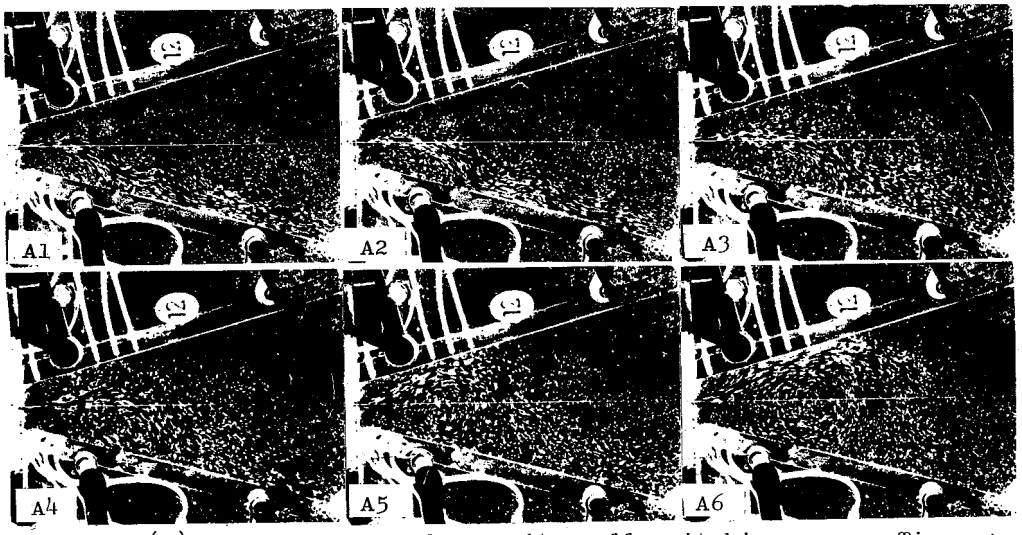

Photo.3(b) Flow patterns of opposite wall switching Time →

Phase 2 follows phase 1 and ends when the jet attaches to the opposite side wall.

Phase 3 follows phase 2 and ends when a pressure signal is obtained in a reciever placed downstream of the fluidic device. During this phase the jet remains as it attaches with both side walls.

"The switching criterion" used above is to determine the minimum control pulse which can switch the jet.

Using the pressure changes in Fig.8(b) and the flow patterns in Photo.3(b), the switching process mentioned above is explained as below. Referring to the pressure change in opposite side, it is noticed that there is a difference in the rate of the pressure change before time A3 and one after time A3. The time when p_N begins to lower may be the time when the jet begins to move from attaching side to opposite

side, or the switching criterion is just satisfied. Thus the phase 1 ends. And then p_N lowers rapidly and the jet attaches to the opposite side wall at time A5. This period is the phase 2. It is considered that the substantial switching ends at this time. After that, the bubble moves downstream, and p_N and p_B become stable after rising momentarily. This time may be defined as the end of the switching.

The dynamic behaviour of jet to relatively small input ($Q_c \simeq Q_{cs}$) is shown in Photo.3(b) and Fig.8(b). That to relatively large input ($Q_c = 2Q_{cs}$) is shown in Photo.3(a) and Fig.8(a), where Q_{cs} is the static switching control flow rate. The comparison between both cases shows that the switching transient to relatively large input may be divided into two phases (phase 1 and phase 3, only).

While, experiments show that the switching process may be analyzed by putting stress on the phase 3 as done by Özgü [5] when a step input is relatively large or the offset is relatively small.

4.2. Formulation of Switching Process

The phase 2 of the three phases mentioned in previous section may be difficult to formulate because of its complexity in the flow pattern as shown in Photo.4. However, admitting the fact that the time of this phase occupies a very little of total switching time and that the switching process can be divided into two phases(phase 1 and phase 3) in case of relatively large input, the formulation of the switching process may be possible as follows:

As the flow pattern at any time can be obtained by the theory in section 3.1, the time of phase 1 can be calculated if the switching criterion is formulated. With consideration of the influence of lowering of pressure in opposite side on the radius of curvature of

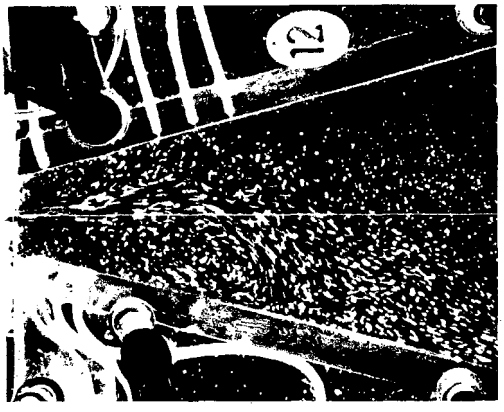

Photo.4 Flow pattern in phase 2

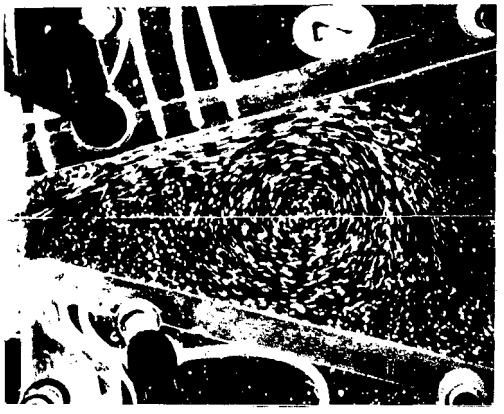

Photo.5 Flow pattern in phase 3

jet R , the switching criterion is given by

$$\frac{d\Delta R}{dx} = -\frac{R^2}{J}\frac{dp_N}{dx} > c, \tag{16}$$

where c is a constant quantity and ΔR is an infinitesimal change of R. The bubble in the phase 3 has a circular region as shown in Photo.5. This photograph means that little flow goes out of the bubble. Therefore, the switching time required the phase 3 can be obtained by the following equation,

$$\frac{dV}{dt} = Q_{in} - Q_{out}, \tag{17}$$

where $Q_{in} = Q_c + Q_s + Q_e$,

$Q_{out} = Q_e$,

and Q_e is the flow rate entrained from the region downstream by the attaching jet. The bubble in this phase is defined by the region enclosed by the attaching streamline and the bounding walls. This attaching streamline is approximated with a circular arc.

The analytical model proposed above can not estimate the time required for the phase 2, but this method has a merit that we can obtain the switching time checking whether the jet switches or not.

The calculated results are compared with the experimental in Fig.10, where τ_1 is the time required for the phase 1, and τ_a is the total switching time. While, for simplifying the analysis, it is assumed that the phase 3 ends when the attaching streamline reaches the end of the fluidic device, as shown in Fig.9. In calculation, c=0.25 is used.

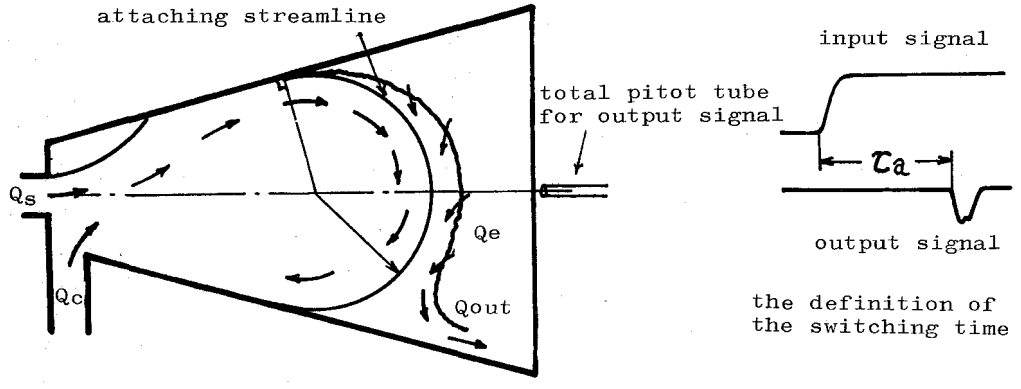

Fig.9 Analytical model for phase 3

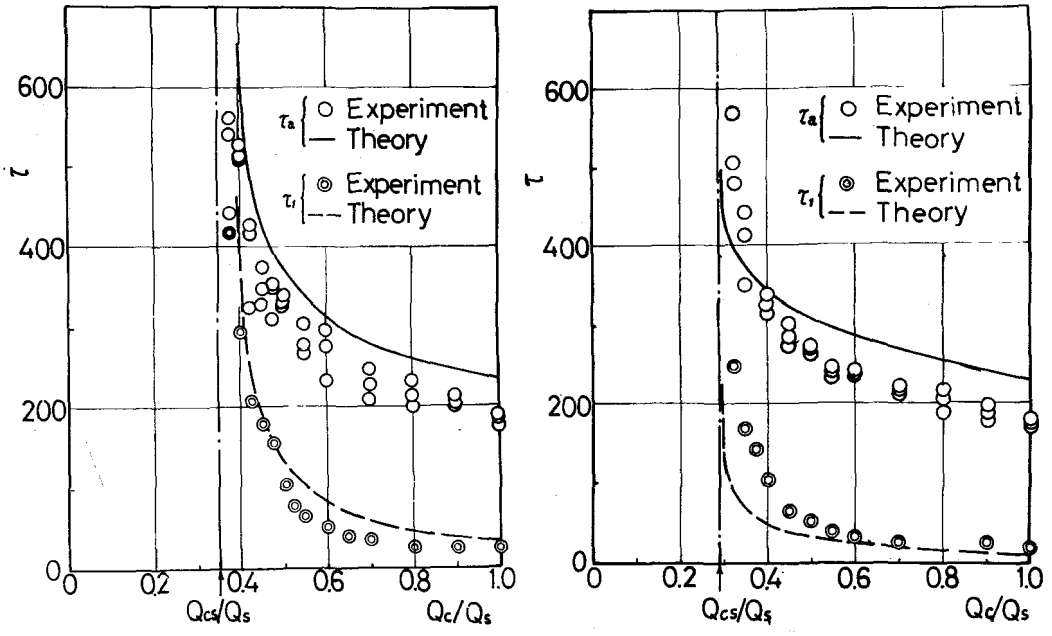

Fig.10 Calculated switching times, compared with experimental

5. Conclusion

The dynamic behaviuor of attaching jet to step control flow was discussed theoretically and experimentally, mainly by means of flow visualization. The results are summarized as follows:

(1) The proposed analytical dynamic model of attaching jet, in which the quasi-steady process is assumed, explains well the dynamic behaviour of attaching jet with single side wall.

(2) The process of the opposite wall switching may be divided into three phases.

(3) Based on the experiments, the analytical model of the opposite wall switching, including the formulation of the switching criterion, was proposed.

Acknowledgement

The authors wish to thank Mr. M. Takagi for his discussion and Mr. K. Ohmori and Mr. T. Yamada for their assistance in experiments.

References

1) H.R. Müller: ASME Paper 64-FE-10 (1964).
2) P.A. Lush: Proc. IFAC Symposium on Fluidics, A3 (1968).
3) M. Epstein: Trans. ASME, Jour. of Basic Engg., 93(1971), 1, 55.
4) T. Wada et al.: Memoirs of School Engg., Okayama Univ., 8(1973), 25.
5) M.R. Özgü & A.H. Stenning: ASME Paper 7-WA/FLCS-6 (1971).
6) T. Wada et al.: Proc. of 2nd Internat. JSME Symposium on Fluid Machinery and Fluidics, 3(1972), 171.

Nomenclature

b_a : half valued width at attachment point
b_s, b_c : nozzle width of main jet and control jet
b_t : potential core width, $(1 - x/x_c)b_s/2$
J : combined jet momentum
J_s^* : momentum through the section BE
J_d : momentum proceeding downstream along attached wall
P_{so} : total pressure of main jet injected into space with uniform ambient pressure
p_D : static pressure in interaction region
p_B : mean pressure in separation bubble
p_N : static pressure in opposite side
Q_e : flow rate entrained from downstream in phase 3
t : time
u_m : maximum velocity on velocity profile
x : distance along jet centerline from main nozzle exit
x_c : potential core length
x_R : attachment distance
V : volume of the bubble
α, α_N : inclined wall angle on attached side and opposite
δ : deflection angle of jet
θ : virtual impingement angle
λ : exchange factor
ξ_a : jet width at attachment point
ρ : fluid density
τ : non-dimensionalized time
$(\bar{\ })$: quantity non-dimensionalized by b_s, P_{so}, Q_s and J_s